ISSN: 2476-6909; Modares. Mech. Eng. *2025;25(05):271-278.*

Modares Mechanical Engineering

DOI: 10.48311/MME.25.5.271
journal homepage: www.mme.modares.ac.ir

Experimental Modeling and Process Optimization of Laser Transmission Welding with Fiber Optic Laser for Polymethyl Methacrylate in Zigzag Path

Milad Rahmaninia* Majid Ghoreishi

Department of Mechanical Engineering, K.N. Toosi University of Technology, Tehran, Iran

ARTICLE INFO

Article Type
Original Research

Article History
Received: February 18, 2025
Revised: May 21, 2025
Accepted: May 28, 2025
ePublished: August 11, 2025

ABSTRACT

Polymethyl methacrylate (PMMA) is extensively used in automotive, aerospace, and consumer products industries due to its favorable mechanical characteristics. Laser Transmission Welding (LTW) has recently gained attention as an advanced joining method for creating strong, narrow, and lightweight welds in thermoplastics like PMMA. This study examines the effects of three key process parameters—laser power, welding speed, and scan line spacing—on the LTW performance when bonding two transparent PMMA sheets using a fiber laser along a zigzag path. The main objective is determining the feasibility of practical welding at low laser power while achieving high joint strength. Experimental design and optimization were conducted using Analysis of Variance (ANOVA) and Response Surface Methodology (RSM). ANOVA confirmed that all three parameters significantly influenced lap-shear force. RSM results showed that higher laser power, lower welding speed, and reduced scan line spacing increased heat input and improved weld strength, with a maximum lap-shear force of 1256 N. In contrast, lower laser power, faster welding, and wider spacing reduced heat input and resulted in a minimum strength of 245 N. Desirability-based optimization identified optimal settings of 30 W laser power, 400 mm/s welding speed, and 0.015 mm scan line spacing, predicting a lap-shear force of 1249.2 N with 99.3% confidence. The results demonstrate that zigzag LTW of PMMA is feasible at low power levels, attributed to uniform heat distribution and consistent melting achieved by the zigzag path.

Keywords: Laser Transmission Welding, Polymethyl Methacrylate, Transparent Polymer Welding Parameters, Zigzag Path, Response Surface Methodology (RSM), Optimization

How to cite this article
Rahmaninia M, Ghoreishi M. Experimental Modeling and Process Optimization of Laser Transmission Welding with Fiber Optic Laser for Polymethyl Methacrylate in Zigzag Path. Modares Mechanical Engineering; *2025;25(05):271-278.*

**Corresponding author's email: Milad.rhmnn@email.kntu.ac.ir*
**Corresponding ORCID ID: 0009-0003-9147-8834*

1- Introduction

Polymethyl Methacrylate (PMMA) is a transparent thermoplastic known commercially as Perspex and Plexiglass. Due to its properties, such as high hardness and transparency, corrosion resistance, low weight, and 92% light transmission capability, it is used in many industries, including automotive, aerospace, agriculture, construction, household appliances, optical instruments, and packaging [1,2]. Given the application of PMMA in various industries, joining this material is essential. Laser welding is one of the processes used for joining thermoplastics, and it is utilized in both research and industry. Laser transmission welding (LTW) is a thermal technique used to weld different types of thermoplastics together, as well as attach thermoplastics to metals, ceramics, and composites [3,4]. Laser transmission welding has many advantages over other methods of combining thermoplastics, including flexibility, quick processing time, high processing speed, non-contact operation, cheap production cost, a small heat-affected zone (HAZ), and the ability to achieve high strength. These benefits have been shown in studies [5,6].

The LTW process comprises four stages: laser transmission, heat production, melting, and solidification [7,8]. When the laser beam goes through the see-through polymer, it is absorbed by the absorbing polymer, resulting in a thermal zone at the boundary between the two polymers. Within this region, polymer components undergo a melting process. The molten materials mix due to clamp pressure, connecting the two parts. This bond solidifies when the materials cool down [9]. According to research done by Wang et al., it was shown that the most effective force for combining PMMA polymer parts using the LTW technique to obtain sufficient strength is 20 N [10]. Line energy, together with clamp pressure, is a significant factor that influences the strength of a weld. The relationship between laser power and welding speed, expressed as the power-to-speed per unit length ratio, is known as line energy [11]. Augmenting the laser's strength directly impacts the amount of energy in each line, influencing the density of the laser's energy. Intense power consumption during long-term welding (LTW) generates a higher amount of heat, which in turn causes the polymer to melt more extensively [12]. High levels of laser power may result in the combustion of polymers and an increase in the heat-affected zone (HAZ) region.

On the other hand, using low power for welding might lead to inadequate polymer melting and poor weld strength [13, 14]. The welding speed directly influences the duration of the laser beam's engagement with the base materials during the welding process. Reducing the pace at which welding is performed results in a longer duration of contact and a higher amount of heat transferred. In contrast, a faster welding speed decreases the time for contact and might result in insufficient bonding because of the decreased heat input [15,16]. Nevertheless, it is crucial to ascertain each material's ideal laser power and welding speed, considering its specific qualities and the kind of laser used, to generate a weld of suitable strength [17]. Response Surface Methodology (RSM) is a statistical technique used to construct experiments and create empirical models. It has been used in numerous research to investigate the effects of different factors on outputs such as laser power, weld-seam width, heat input, and the heat-affected zone (HAZ) [18, 19]. Kumar et al. used Response Surface Methodology (RSM) to construct the experiments for optimizing the parameters of Laser Transmission Welding (LTW) in the bonding of two transparent polymers, polymethyl methacrylate and polycarbonate, using a pulsed Nd: YVO4 laser. The use of Desirability Function analysis enhanced the findings. This research examined the effects of many factors on lap-shear force, including laser power, pulse frequency, scanning speed, wobble width, and wobbling frequency. The analysis of variance findings indicates that the wobbling width parameter had the most significant influence on weld strength [20]. Acherjee et al. researched the laser transmission welding of two polymers, PMMA and ABS, using RSM modeling. This study used a diode laser with a wavelength of 809.4 nm. The influence of four factors, including laser power, welding speed, stand-off distance, and clamp pressure, on weld strength was assessed. The analysis of variance data determined that the stand-off distance had the most significant impact on the strength [17].

The evaluation of weld quality relies heavily on the essential criteria of weld strength [9]. The criterion used to assess the strength of welds in lap joint connections is the shear force exerted by the tensile testing equipment on the weld joint [21,22]. The mode of weld zone failure under shear stress is crucial in determining the appropriate range of factors that impact weld strength. Surface and substrate damage are prevalent problems in components connected using the LTW technique. If the weld joint sustains damage, it is classified as surface damage. Surface damage indicates lower weld strength compared to the underlying material. However, if the harm arises from the region next to the weld joint, it is referred to as substrate damage. Substrate damage suggests that the weld connection is stronger than the base material [23, 24]. Hence, it is essential to contemplate an optimum combination of factors to get the highest possible weld strength [25,26]. Controlling the LTW process optimizes and minimizes faults in the joint region and ensures that the parameters influencing weld strength width are within the proper range [27, 28]. Temperature measurement throughout the LTW process yields data on the amount of heat applied to the weld zone, the extent of polymer melting, and the range of the heat-affected zone (HAZ) [29]. Pyrometry is a contactless technique used to measure the temperature in the LTW process. Due to the rapid heat transfer rate in LTW and the possibility of measurement inaccuracies when employing Pyrometry to determine the temperature in the weld zone, it is necessary for both the heat input temperature to the weld zone and the emitted temperature from this region to be relatively high [30, 31].

The current study thoroughly analyzes the effects of a zigzag laser beam path and three adjustable parameters (laser power, welding speed, and distance between scan lines) on the strength of the weld between two transparent PMMA polymer pieces. This analysis was conducted through experimental investigation, empirical modeling, and process optimization.

This study explores the potential of achieving high-strength joints between two transparent PMMA components using Laser Transmission Welding (LTW) with a low-power laser following a zigzag scanning path. The research evaluates the effects of three controllable parameters—laser power, welding speed, and distance between scan lines—on weld strength. These parameters were optimized using Response Surface Methodology (RSM) alongside Desirability Function analysis. A low-power fiber laser with beam-scanning capabilities performed the LTW process. A black ink coating was applied to the joint area as an absorptive layer to promote efficient laser absorption, localized heating, and proper molten pool formation at the bonding interface.

Additionally, a novel application of Pyrometry was implemented to estimate weld-zone temperature, enabling the identification of suitable processing conditions in the early experimental stages without requiring immediate mechanical testing. RSM and Analysis of Variance (ANOVA) were employed to systematically design the experiments, identify key influencing parameters, and develop a predictive relationship between input factors and Lap-shear strength. The optimal combination of process parameters was ultimately determined, resulting in the maximum lap-shear force, as verified by the desirability-based optimization approach.

2-Experimental methods and details

2.1.Material and process

Transparent PMMA sheets with dimensions of 80 mm × 35 mm × 4 mm were prepared for this experimental study. The physical properties of this polymer are presented in Table 1. For the LTW process, a Raycus_50QB fiber marking laser machine with a

maximum power of 50 W, a wavelength of 1064 nm, an adjustable speed of up to 7000 mm/s, an adjustable frequency range of 50-100 kHz, and a computer connected to the laser machine was used. Parameter settings for each welding stage were adjusted using the EZ-CAD software available on the computer connected to the laser machine. This laser device transmits the laser beam via an optical fiber cable from the laser source to the laser head. To remove dust and other surface impurities, all sample surfaces were cleaned with ethyl alcohol. To absorb the laser beam, the surface of half of the workpieces was coated with ink. Before welding, the surfaces were dried with warm air to eliminate surface moisture. The welding process of PMMA samples is shown in Figure 1a, and a welded PMMA sample is shown in Figure 1b.

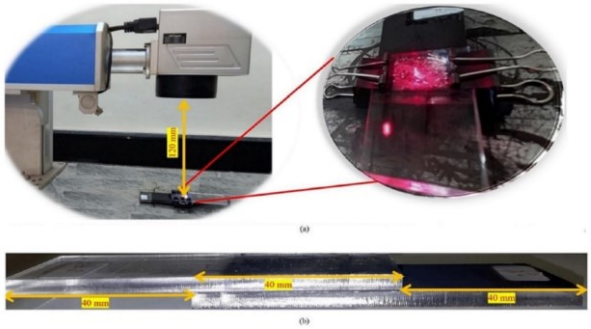

Fig. 1 a) View of fiber optic laser welding PMMA b) Welded PMMA sample

Table 1 Physical and mechanical properties of Poly methyl methacrylate [32]

Property	PMMA
Density (g/cm³)	1.18
Melting Point (°C)	220-240
Surface Hardness (Rockwell)	M92, M90, M100
Glass Transition Temp (Tg)	110 to 120
Linear Thermal Expansion (× 10^{-5} mm/mm.k)	6.3
Thermal Conductivity at 20 °C (KW/mk)	0.12 - 0.17
Refractive index	1.49
Luminance transmission	92%
Tensile Strength (MPa)	72
Tensile Modulus (GPa)	3.1

Wang et al. [10] reported that a minimum clamping force of 20 N is necessary to achieve proper adhesion and prevent air infiltration at the joint interface of two PMMA components. Accordingly, two mechanical clamps (Figure 2) were used to apply the required compressive force to the samples during welding. A piezoelectric force sensor integrated with an Arduino board accurately measured and monitored the applied clamping force.

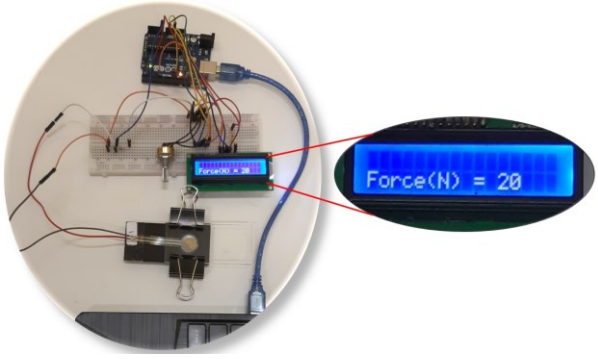

Fig. 2 Method of measuring the clamping force.

2.2 Testing process

Preliminary tests indicated that welding temperatures significantly lower or higher than PMMA's melting point led to inadequate joint formation. At lower temperatures, insufficient heat generation resulted in poor melting and weak bonding between the parts. On the other hand, excessive temperatures caused thermal degradation or vaporization of PMMA, which disrupted the fusion of polymer chains and prevented the formation of a strong weld. Therefore, the selection of both fixed and variable process parameters was guided by the goal of maintaining welding temperatures close to the PMMA melting point. Pyrometry was employed during the welding process to monitor the thermal behavior of the weld zone and confirm that the welding occurred within this critical temperature range. This non-contact temperature measurement technique provided real-time feedback, enabling proper adjustment of parameters and avoiding the need for destructive testing in early experimental stages.

Due to the substantial heat transfer, accurately measuring the temperature of the weld zone in the Laser Transmission Welding (LTW) process is a challenge. Therefore, it is impractical to measure the weld area's temperature using pyrometry precisely. Pyrometry, however, may be an appropriate technique for visually examining and determining the range of input parameters for research purposes. Therefore, a pyrometer with a temperature range from -35 to 500 degrees Celsius and a precision of 0.1 degrees Celsius was used to estimate the temperature of the weld zone and determine the acceptable range of input parameters.

The strength of the welded PMMA pieces increases proportionally with the magnitude of the shear force they can endure. Consequently, a tensile test was used to evaluate the strength of the weld. The testing machine has a maximum capacity of 2.5 tons. As per the ASTM D 1002 standard, the upper and lower jaws of the tensile testing equipment held the welded sample, with 2.5 cm measured from each direction. The welded samples underwent a tensile test at a temperature of 25°C, with a speed of 0.5 mm/min.

2.3 Experimental design

2.3.1 OFAT Method

In the initial stage of the experiments, real-time temperature monitoring was conducted using pyrometry, and the One-Factor-at-a-Time (OFAT) approach was applied to determine both constant and variable input parameters that facilitate the practical welding of PMMA samples within the material's melting temperature range. Based on the results of these preliminary tests, three variable parameters—laser power, welding speed, and distance between scan lines —were identified as significantly impacting the Lap-shear force in the zigzag welding configuration. Each of these variables was investigated at three different levels, all chosen to maintain the process within the optimal thermal range near PMMA's melting point, as detailed in Table 2. Additionally, three parameters—Focal Point Position (FPP), Laser pulse frequency, and Clamping force—were held constant throughout the experiments to limit the number of test conditions and reduce overall experimental costs. The fixed values for these parameters were set as follows: a focal distance of 120 mm, a pulse frequency of 50 kHz, and a clamping force of 20 N.

2.3.2 RSM Method

Response Surface Methodology (RSM) is a collection of mathematical and statistical tools used to model and analyze issues in which the output of interest is affected by many input factors. The goal is to maximize the efficiency of the reaction. The outcome of this procedure yields a regression equation (Equation 1) that precisely defines the connection between the input parameters (χ) and the response variable (y). The equation may be described as follows: y represents the response, χ represents the independent variables, β represents the regression coefficients, and ε represents the observed error [33].

$$y = \beta_0 + \sum_{i=1}^{k} \beta_i x_i + \sum_{i=1}^{k} \beta_{ii} x_i^2 + \sum_i \sum_j \beta_{ij} x_i x_j + \varepsilon \quad (1)$$

To design the experiments and optimize the process variables, this study employed Response Surface Methodology (RSM) in conjunction with a face-centered central composite design (FCCD). This statistical approach was chosen due to its widespread application and proven effectiveness in producing accurate, high-quality results while minimizing the required experimental runs. The input parameters investigated were laser power, welding speed, and distance between scan lines, each tested at three defined levels to evaluate their individual and combined effects on the welding process. The specific parameter levels used in the study are detailed in Table 2.

Table 2 Process control parameters and their limits.

Input Parameters (Controllable)	Unit	Notations	Level		
			-1	0	+1
Laser power (A)	Watt	P	20	25	**30**
Welding speed (B)	$\frac{mm}{s}$	V	400	425	**450**
distance between scan lines (C)	mm	LD	0.015	0.02	**0.025**

2.3.3 Optimization using examination of desirability functions.

The Derringer and Suich optimization methodology is viable for simultaneously optimizing several outputs [34]. This approach relies on Desirability functions. Under this methodology, every output y_i is first transformed into a desirability function di, which spans from zero to one ($0 \leq d_i \leq 1$). Within this function, when the output y_i matches the desired value, the variable di is assigned a value of 1. Conversely, if the output falls beyond the allowed range, di is assigned a value of 0. The input variables are chosen to optimize the total desirability D [33].

3. Results and Discussion

3.1 Development of mathematical models

The Minitab version 21.4.2 (64-bit) Software was used to assess and generate an appropriate regression equation for fitting the collected data. Before the analysis of variance, tests were performed in the order of the results presented in Table 3 to remove factor noise. The ANOVA approach was used to assess the significance or insignificance of the input parameters. In this approach, the F-value and lack of fit were used to assess and examine the efficacy or ineffectiveness of the input parameters, as well as the correctness and sufficiency of the model.

3.1.1 Analysis of Lap-shear Force

The purpose of the regression equation is to construct a coherent link between the response variable and the independent input factors. Equation 2 is the regression equation that reflects the output shear force. Table 4 displays the R^2, corrected R^2, and anticipated R^2 values, as well as other indicators of adequacy for the shear force. The proximity of the R^2, adjusted R^2, and predicted R^2 values to one suggests that the model is efficient. Based on the data in the table, if the input parameters have a P-value lower than 0.05 (α=0.05, or 95% confidence level), they significantly affect the shear force with a confidence level above 95%. If any input parameters have a P-value that exceeds 0.05, they lack significance.

Furthermore, a model is deemed satisfactory if the lack-of-fit value exceeds 0.05. The ANOVA table indicates that the variables Laser power (P), welding speed (S), the distance between scan lines (LD), the quadratic effect of laser power (P^2), the quadratic effect of welding speed (S^2), the interaction effect of laser power and welding speed (P×S), and the interaction effect of welding speed and distance between scan lines (S×LD) significantly influence the lap shear force. Out of all the input parameters, the one with the most influence on the lap shear force is laser power, with an F-value of 1598.31. On the other hand, the parameter with the least influence is the quadratic effect of welding speed (S^2) with an F-value of 5.36. The parameters (LD^2), representing the quadratic effect of the distance between scan lines, and (P×LD), representing the interaction effect of laser power and distance between scan lines, were eliminated from the model since they have no impact on the shear force and their removal was done to enhance the model.

Table 3 Design matrix and measured responses.

Experimental information					Results
Run order	Std order	Welding Parameters			
		P (watt)	S ($\frac{mm}{s}$)	LD (mm)	**Lap-shear Force (N)**
1	2	30	425	0.020	**1025**
2	37	20	450	0.025	**245**
3	30	20	400	0.015	**875**
4	25	30	450	0.015	**1044**
5	3	30	400	0.025	**936**
6	35	25	425	0.020	**664**
7	32	25	400	0.020	**792**
8	8	25	425	0.020	**655**
9	9	20	400	0.025	**585**
10	38	25	425	0.020	**670**
11	1	25	425	0.025	**542**
12	40	20	450	0.015	**472**
13	5	30	400	0.015	**1256**
14	12	30	450	0.025	**785**
15	16	20	425	0.020	**580**
16	23	25	425	0.020	**695**
17	33	25	425	0.015	**845**
18	14	25	425	0.020	**710**
19	36	25	425	0.020	**660**
20	18	25	450	0.020	**530**

The graphs shown in Figure 3 examine the influence of each input parameter. Increasing the laser power (P) from 20 W to 30 W resulted in higher temperatures in the weld region and enhanced polymer melting. Upon reaching their critical temperatures, the absorbing and transparent polymers underwent melting, resulting in an expansion in the volume of the molten fluid. Consequently, there was an increased degree of intermingling and adhesion among the polymer molecules. Consequently, a stronger bond between the two polymers was established after they hardened. Increasing the welding speed (S) led to a decrease in the temperature of the weld zone, hence lowering the amount of polymer melt in that area. Consequently, the weld strength decreased when the welding speed increased from 400 mm/s to 450 mm/s. The distance between scan lines (LD) directly impacts the quantity of laser beam scans inside a particular area. Consequently, reducing the distance between the scan lines of the beam resulted in an increased number of laser beam scans on the surface under

examination. Increasing the number of laser beam scans on a surface resulted in higher temperatures in the weld zone, increasing the polymer's melting in that area. Consequently, the weld strength decreased as the distance between scan lines rose from 0.015 mm to 0.025 mm.

$$\begin{aligned} F\,Zigzag = {} & 3691 - 351.8 \\ & P + 14.4S - 80680 \\ & LD + 4.723 \\ & P \times P - 0.0375 \\ & S \times S + 0.38 \\ & P \times S + 124\ \ S \times LD \end{aligned} \qquad (2)$$

Table 4 ANOVA analysis for the lap-shear Force width model (after backward elimination).

Source	DF	Sum of squares	Mean squares	F-value	P-value	
Model	7	982624	140375	428.21	0.000	**Significant**
Linear	3	906815	302272	922.08	0.000	
P	1	523952	523952	1598.31	0.000	
S	1	187142	187142	570.88	0.000	
LD	1	195720	195720	597.04	0.000	
Square	2	55838	27919	85.17	0.000	
P*P	1	44604	44604	136.06	0.000	
S*S	1	1758	1758	5.36	0.039	
2-Way Interaction	2	19972	9986	30.46	0.000	
P*S	1	18050	18050	55.06	0.000	
S*LD	1	1922	1922	5.86	0.032	
Error	12	3934	328			
Lack-of-Fit	7	1540	220	0.46	0.830	**Not Significant**
Pure Error	5	2393	479			
Total	19	986558				
R^2= 99.60%	Adjusted R^2= 99.37%			**Predict R^2= 98.99%**		

3.2 Effects of process parameters on the responses

3.2.1. Main Effects Plots for Lap-shear Force

The graphs shown in Figure 3 examine the influence of each input parameter. Increasing the laser power (P) from 20 W to 30 W resulted in higher temperatures in the weld region and enhanced polymer melting. Upon reaching their critical temperatures, the absorbing and transparent polymers underwent melting, resulting in an expansion in the volume of the molten fluid. Consequently, there was an increased degree of intermingling and adhesion among the polymer molecules. Consequently, a stronger bond between the two polymers was established after they hardened. Increasing the welding speed (S) led to a decrease in the temperature of the weld zone, hence lowering the amount of polymer melt in that area. Consequently, the weld strength decreased when the welding speed increased from 400 mm/s to 450 mm/s. The distance between scan lines (LD) directly impacts the quantity of laser beam scans inside a particular area. Consequently, reducing the distance between the scan lines of the beam resulted in an increased number of laser beam scans on the surface under examination. Increasing the number of laser beam scans on a surface resulted in higher temperatures in the weld zone, increasing the polymer's melting in that area. Consequently, the weld strength decreased as the distance between scan lines rose from 0.015 mm to 0.025 mm.

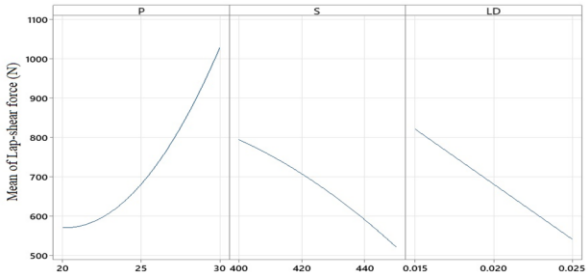

Fig. 3 Main Effects Plots for Lap-shear force.

3.2.2. Interaction Plots for Lap-shear Force

Concurrently augmenting laser intensity and reducing welding velocity results in a rise in line energy [15]. Inadequate fusion or weak weld strength occurs due to low line energy, while excessive line energy leads to polymer base materials being burned and degraded. Thus, it is necessary to determine the most favorable energy level for the line energy. To achieve uniform line energy across all levels of laser power and welding speed, one may raise both power and speed or reduce both simultaneously. This method achieves a uniform heat input in the welding area after attaining the ideal line energy.

As illustrated in Figure 4, the interaction between laser power and welding speed significantly influences the line energy, affecting weld quality. Increased laser power at lower welding speeds leads to higher line energy and more extensive melting within the weld zone. This condition enhances joint formation and increases the resulting Lap-shear force. Notably, changes in laser power exhibit a more substantial impact on line energy—and thus on weld strength—than variations in welding speed alone. For instance, under maximum laser power (30 W) and minimum welding speed (400 mm/s), the Lap-shear force exceeded 1000 N. In contrast, at the lowest laser power (20 W) and highest welding speed (450 mm/s), the Lap-shear force decreased to just above 400 N.

Further analysis of the interaction between welding speed and distance between scan lines (S × LD), as shown in Figure 4, indicates that decreasing both parameters simultaneously increases the heat input into the weld area, thereby strengthening the joint. Conversely, increasing both parameters reduces the heat input and the Lap-shear force. The nearly symmetrical variation in Lap-shear force observed across these parameter combinations suggests that welding speed and distance between scan lines exert comparable influence on joint strength. When welding speed and distance between scan lines were at their minimum levels (400 mm/s and 0.015 mm, respectively), the Lap-shear force approached 1000 N. However, increasing these to their maximum levels (450 mm/s and 0.025 mm) led to a significant reduction in Lap-shear force, with values around 400 N. According to ANOVA results, the interaction between laser power and distance between scan lines (P × LD) did not statistically affect Lap-shear force. Consequently, this interaction was excluded from the plots presented in Figure 4.

3.2.3. Contours plot and Response surface plots for Lap-shear force

Figure 5 displays the contour and planar graphs illustrating the changes in shear force due to the combined influence of laser power and welding speed (P×S). The beamline parameter distance in these photos is set to its center value of 0.02 mm. Figure 5(a) demonstrates that increasing laser power and reducing welding speed increased weld strength. This is caused by the higher amount of heat being applied to the area where the weld is being made, which is influenced by the changing energy levels along the weld line. The maximum heat input to the weld zone was at a laser power of around 29-30 W, with a welding speed ranging from 400-435 mm/s.

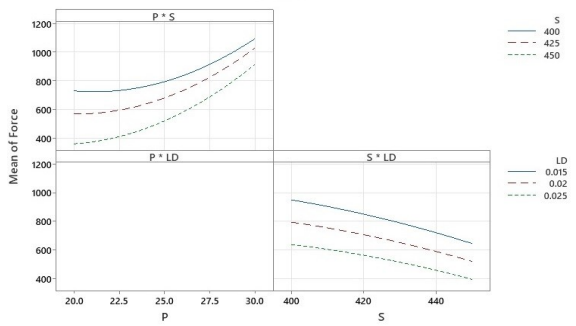

Fig. 4 Interaction Plots for Lap-shear force.

In contrast, diminishing the laser power and augmenting the welding speed resulted in a loss in line energy, which led to a reduction in heat input to the weld zone, a decrease in polymer melting, and, therefore, a decline in weld strength. The minimum shear force values were observed when the laser power ranged from around 20-23 W, and the welding speed varied from around 448-450 mm/s. The planar graph in Figure 5(b) illustrates the correlation between line energy and heat input on weld strength. It demonstrates that shear pressures exceeding 1000 N were attained when the line energy reached its highest point. Figures 6(a) and 6 (b) show the contour and planar graphs illustrating the changes in shear force resulting from the interaction between welding speed and the distance between scan lines (S×LD). In this case, the laser power remains constant at its center value of 25 W. Figure 6(a) demonstrates that reducing the welding speed and the distance between scan lines simultaneously increased the lap-shear force. Thus, it can be inferred that a decrease in the interaction effect of welding speed and the distance between scan lines (S×LD) increases the heat input to the weld zone. Enhanced thermal transfer, generating a suitable amount of molten material substance, integrating the base material, and eventually creating a robust connection in the welding area are further consequences of amplifying the interaction effect of welding speed and the distance between scan lines (S×LD). The optimal welding speed range for achieving the most significant shear force in a zigzag route is around 400-410 mm/s, while the recommended distance between scan lines is around 0.015-0.016 mm.

In contrast, the optimal values for minimizing lap-shear force are 435-450 mm/s and 0.023-0.025 mm. Based on the data shown in Figure 6(b), it was found that while using a laser power of 25 W, no welds were seen to have a shear strength of more than 1000 N. The laser power parameter substantially impacts the heat input to the weld zone compared to the welding speed, distance between scan lines, and their interaction effect. Consequently, shear strengths greater than 1000 N were observed when the laser power reached 30 W.

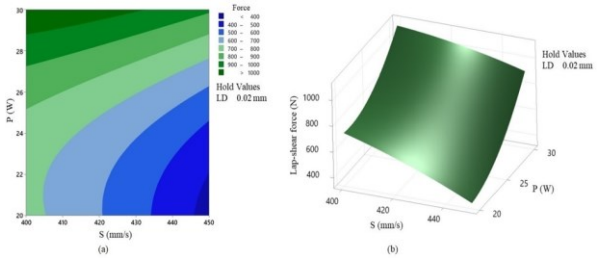

Fig. 5 (a) Contours plot and (b) response surface plot showing the effect of P and S on the lap-shear force that LD= 0.02 mm.

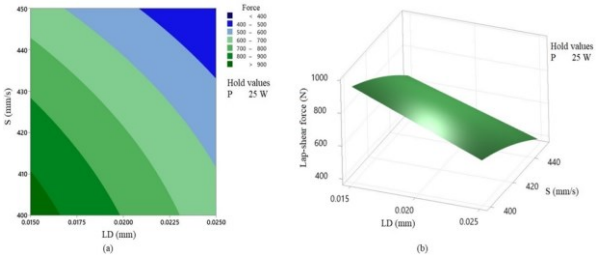

Fig. 6 (a) Contours plot and (b) response surface plot showing the effect of S and LD on the lap-shear force that P= 25 W.

4. Optimization of Lap shear force

The process output was optimized by adjusting the parameters to achieve optimum weld strength. Fig.7 presents the process parameters arranged in columns, where each row represents different output variations. Every individual cell demonstrates the changes in the corresponding output when the input parameters are modified. The values at the top of each column represent each parameter's high, optimal, and low settings, respectively. The optimization findings indicate that the ideal parameter values are a laser power of 30 W, a welding speed of 400 mm/s, and a beam distance of 0.015 mm. The first cell of each row displays the forecasted output value and its corresponding probability of attainment. Based on the projected model, if welding is repeated using these ideal parameters, the welded samples will exhibit a maximum tensile strength of 1249.21 N. The findings suggest that the given optimum values are satisfactory, as shown by a Desirability Function score of 99.3%.

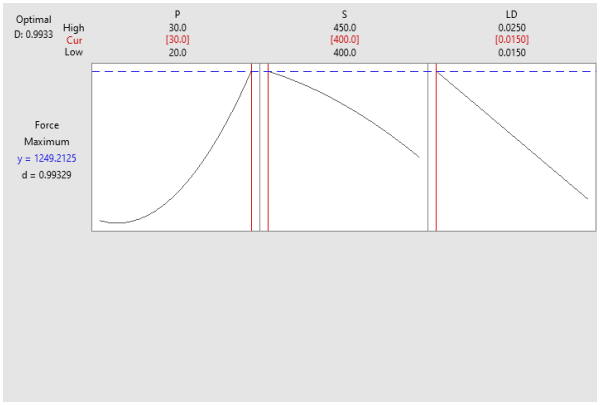

Fig. 7 Optimization plot for weld lap shear force.

5 .Conclusion

Transparent PMMA samples were joined using a low-power fiber laser through a transmission welding process along a zigzag scanning path. The zigzag pattern contributed to a uniform heat distribution across the weld zone, facilitating consistent molten flow and enhancing joint strength. Notably, this welding configuration formed strong joints at low laser power and high scanning speeds, characterized by low line energy. Reducing laser power and increased welding speed led to lower line energy, reducing heat input and the weld zone temperature. When the temperature dropped below the melting point of PMMA, incomplete melting occurred, weakening joint strength. Conversely, excessive line energy caused overheating, polymer over-melting, and material vaporization and degradation, negatively impacting weld integrity. These findings underscore the importance of optimizing line energy to ensure high-strength welds. Another influential factor was the distance between scan lines. Decreasing this parameter increased the welding time and heat input, promoting more thorough polymer melting and, thus, stronger joints. According to the ANOVA results, among the three investigated parameters—laser power, welding speed, and distance between scan

lines —laser power emerged as the most significant factor affecting Lap-shear force and overall weld quality. The highest recorded Lap-shear force was 1256 N, achieved under the optimal 30 W laser power combination, 400 mm/s welding speed, and 0.015 mm scan line distance. Based on desirability function analysis, applying these optimal parameters yields an estimated Lap-shear force of 1249.21 N with a 99.3% probability, demonstrating the reliability and repeatability of the proposed welding strategy.

Ethical Statement

The content of this manuscript is original, based on the authors' research, and has not been published or submitted elsewhere, either in Iranian or international journals.

Conflict of interest

The authors declared that they have no conflicts of interest to this work.

Refrences

[1] S. Prakash and S. Kumar, Determining the suitable CO2 laser based technique for microchannel fabrication on PMMA, Optics & Laser Technology, vol. 139, p. 107017, (2021). https://doi.org/10.1016/j.optlastec.2021.107017.

[2] Y. Huang, X. Gao, B. Ma and Y. Zhang, Interface formation and bonding mechanisms of laser welding of PMMA plastic and 304 austenitic stainless steel, Metals, vol.11, p. 1495, (2021). https://doi.org/10.3390/met11091495

[3] Y. Luan, J. Liu and Y. Shi, Effect of surface texture on quality of stainless steel-PET transmission welding, Optics & Laser Technology, vol. 161, p. 109144, (2023). https://doi.org/10.1016/j.optlastec.2023.109144

[4] S. Wang, W. Wang, Y. Xu, Y. Tian, X. Zhang and H. Huang, Enhancing bonding synergy and mechanical response of metal/composite hybrid joints through physicochemical surface pretreatment, Journal of Materials Processing Technology, vol. 315, p. 117923, (2023). https://doi.org/10.1016/j.jmatprotec.2023.117923

[5] B. Acherjee, Laser transmission welding of polymers–a review on process fundamentals, material attributes, weldability, and welding techniques, Journal of Manufacturing Processes, vol. 60, pp. 227-246, (2020). https://doi.org/10.1016/j.jmapro.2020.10.017

[6] M. Brosda, P. Nguyen, A. Olowinsky and A. Gillner, Analysis of the interaction process during laser transmission welding of multilayer polymer films with adapted laser wavelength by numerical simulation and thermography, Journal of Laser Applications, vol. 32, (2020). https://doi.org/10.2351/7.0000113

[7] E. Ghorbel, G. Casalino and S. Abed, Laser diode transmission welding of polypropylene: Geometrical and microstructure characterisation of weld, Materials & Design, vol. 30, pp. 2745-2751, (2009). https://doi.org/10.1016/j.matdes.2008.10.027

[8] N. Kumar and A. Bandyopadhyay, A state-of-the-art review of laser welding of polymers-part I: welding parameters, Welding Journal, vol. 100, pp. 221-228, (2021). https://doi.org/10.29391/2021.100.019

[9] B. Acherjee, Laser transmission welding of polymers–a review on welding parameters, quality attributes, process monitoring, and applications, Journal of Manufacturing Processes, vol. 64, pp. 421-443, (2021). https://doi.org/10.1016/j.jmapro.2021.01.022

[10] X. Wang, B. Liu, W. Liu, X. Zhong, Y. Jiang and H. Liu, Investigation on the mechanism and failure mode of laser transmission spot welding using PMMA material for the automotive industry, Materials, vol. 10, p. 22, (2017). https://doi.org/10.3390/ma10010022

[11] E. Haberstroh and W. Hoffmann, Laser transmission welding of complex micro plastic parts, Proceedings of the Institution of Mechanical Engineers, Part B: Journal of Engineering Manufacture, vol. 222, pp. 47-54, (2008). https://doi.org/10.1243/09544054JEM842

[12] X. Wang, X. Zhong, W. Liu, B. Liu and H. Liu, Investigation on enhancement of weld strength between PMMA and PBT in laser transmission welding—Using intermediate material, Journal of Applied Polymer Science, vol. 133, (2016). https://doi.org/10.1002/app.44167

[13] A. Gisario, F. Veniali, M. Barletta, V. Tagliaferri and S. Vesco, Laser transmission welding of poly (ethylene terephthalate) and biodegradable poly (ethylene terephthalate)–based blends, Optics and Lasers in Engineering, vol. 90, pp. 110-118, (2017). https://doi.org/10.1016/j.optlaseng.2016.10.010

[14] P. Bates, T. Okoro and M. Chen, Thermal degradation of PC and PA6 during laser transmission welding, Welding in the World, vol. 59, pp. 381-390, (2015). https://doi.org/10.1007/s40194-014-0209-9

[15] B. Acherjee, D. Misra, D. Bose and K. Venkadeshwaran, Prediction of weld strength and seam width for laser transmission welding of thermoplastic using response surface methodology, Optics & Laser Technology, vol. 41, pp. 956-967, (2009). https://doi.org/10.1016/j.optlastec.2009.04.007

[16] B. Acherjee, A. S. Kuar, S. Mitra and D. Misra, Modeling of laser transmission contour welding process using FEA and DoE, Optics & Laser Technology, vol. 44, pp. 1281-1289, (2012). https://doi.org/10.1016/j.optlastec.2011.12.049

[17] B. Acherjee, A. S. Kuar, S. Mitra, D. Misra and S. Acharyya, Experimental investigation on laser transmission welding of PMMA to ABS via response surface modeling, Optics & Laser Technology, vol. 44, pp. 1372-1383, (2012). https://doi.org/10.1016/j.optlastec.2011.12.029

[18] F. Dave, M. M. Ali, M. Mokhtari, R. Sherlock, A. McIlhagger and D. Tormey, Effect of laser processing parameters and carbon black on morphological and mechanical properties of welded polypropylene, Optics & Laser Technology, vol. 153, p. 108216, (2022). https://doi.org/10.1016/j.optlastec.2022.108216

[19] A. S. Bideskan, P. Ebrahimzadeh and R. Teimouri, Fabrication of bi-layer PMMA and aluminum 6061-T6 laminates by laser transmission welding: Performance prediction and optimization, International Journal of Lightweight Materials and Manufacture, vol. 3, pp. 150-159, (2020). https://doi.org/10.1016/j.ijlmm.2019.09.008

[20] D. Kumar, N. S. Sarkar, B. Acherjee and A. S. Kuar, Beam wobbling effects on laser transmission welding of dissimilar polymers: Experiments, modeling, and process optimization, Optics & Laser Technology, vol. 146, p. 107603, (2022). https://doi.org/10.1016/j.optlastec.2021.107603

[21] B. Acherjee, A. S. Kuar, S. Mitra and D. Misra, Empirical modeling and multi-response optimization of laser transmission welding of polycarbonate to ABS,

Lasers in Manufacturing and Materials Processing, vol. 2, pp. 103-123, (2015). https://doi.org/10.1007/s40516-015-0009-0.
[22] T. B. Juhl, D. Bach, R. G. Larson, J. d. Christiansen and E. A. Jensen, Predicting the laser weldability of dissimilar polymers, Polymer, vol. 54, pp. 3891-3897, (2013). https://doi.org/10.1016/j.polymer.2013.05.053
[23] N. Amanat, C. Chaminade, J. Grace, D. R. McKenzie and N. L. James, Transmission laser welding of amorphous and semi-crystalline poly-ether–ether–ketone for applications in the medical device industry, Materials & design, vol. 31, pp. 4823-4830, (2010). https://doi.org/10.1016/j.matdes.2010.04.051
[24] B. Acherjee, A. S. Kuar, S. Mitra and D. Misra, Application of grey-based Taguchi method for simultaneous optimization of multiple quality characteristics in laser transmission welding process of thermoplastics, The International Journal of Advanced Manufacturing Technology, vol. 56, pp. 995-1006, (2011). https://doi.org/10.1007/s00170-011-3224-7
[25] B. Acherjee, A. S. Kuar, S. Mitra and D. Misra, Effect of carbon black on temperature field and weld profile during laser transmission welding of polymers: A FEM study, Optics & Laser Technology, vol. 44, pp. 514-521, (2012). https://doi.org/10.1016/j.optlastec.2011.08.008
[26] B. Acherjee, 3-D FE heat transfer simulation of quasi-simultaneous laser transmission welding of thermoplastics, Journal of the Brazilian Society of Mechanical Sciences and Engineering, vol. 41, p. 466, (2019). https://doi.org/10.1007/s40430-019-1969-3
[27] W. Horn, A progressive laser joining method: online process control with pyrometer and galvo scanner, vol. 6, ed: Wiley Online Library, pp. 42-43, (2009). https://doi.org/10.1002/latj.200990008
[28] A. Schmailzl, S. Steger and S. Hierl, Process Monitoring at Laser Welding of Thermoplastics: 3D-scanner with integrated pyrometer enables online temperature monitoring at quasi-simultaneous laser transmission welding, Laser Technik Journal, vol. 12, pp. 34-37, (2015). https://doi.org/10.1002/latj.201500029
[29] M. Villar, C. Garnier, F. Chabert, V. Nassiet, D. Samélor, J. C. Diez, et al., In-situ infrared thermography measurements to master transmission laser welding process parameters of PEKK, Optics and Lasers in Engineering, vol. 106, pp. 94-104, (2018). https://doi.org/10.1016/j.optlaseng.2018.02.016
[30] V. Wippo, M. Devrient, M. Kern, P. Jaeschke, T. Frick, U. Stute, et al., Evaluation of a pyrometric-based temperature measuring process for the laser transmission welding, Physics Procedia, vol. 39, pp. 128-136, (2012). https://doi.org/10.1016/j.phpro.2012.10.022
[31] A. Schmailzl, J. Käsbauer, J. Martan, P. Honnerová, F. Schäfer, M. Fichtl, et al., Measurement of core temperature through semi-transparent polyamide 6 using scanner-integrated pyrometer in laser welding, International Journal of Heat and Mass Transfer, vol. 146, p.118814,(2020).https://doi.org/10.1016/j.ijheatmasstransfer.2019.118814
[32] U. Ali, K. J. B. A. Karim and N. A. Buang, A review of the properties and applications of poly (methyl methacrylate)(PMMA), Polymer Reviews, vol. 55, pp. 678-705,(2015). https://doi.org/10.1080/15583724.2015.1031377
[33] W. A. Jensen, Response surface methodology: process and product optimization using designed experiments 4th edition, ed: Taylor & Francis, (2017). https://doi.org/10.1080/00224065.2017.11917988
[34]G. Derringer and R. Suich, Simultaneous optimization of several response variables, Journal of quality technology, vol. 12, pp. 214-219, (1980). https://doi.org/10.1080/00224065.1980.11980968
[35] X. F. Xu, P. J. Bates and G. Zak, Effect of glass fiber and crystallinity on light transmission during laser transmission welding of thermoplastics, Optics & Laser Technology, vol. 69, pp. 133-139, (2015). https://doi.org/10.1016/j.optlastec.2014.12.025
[36] C. Wang, P. Bates and G. Zak, Optical properties characterization of thermoplastics used in laser transmission welding: scattering and absorbance, Advanced Materials Research, vol. 97, pp. 3836-3841, (2010). https://doi.org/10.4028/www.scientific.net/AMR.97-101.3836
[37] J. Coelho, M. Abreu and M. Pires, High-speed laser welding of plastic films, Optics and lasers in engineering, vol. 34, pp. 385-395, (2000). https://doi.org/10.1016/S0143-8166(00)00071-3
[38] E. Braun and B. C. Levin, Nylons: A review of the literature on products of combustion and toxicity, Fire and materials, vol. 11, pp. 71-88, (1987). https://doi.org/10.1002/fam.810110204
[39] H. Liu, H. Jiang, D. Guo, G. Chen, Z. Yan, P. Li, et al., Study on welding mechanism based on modification of polypropylene for improving the laser transmission weldability to PA66, Materials, vol. 8, pp. 4961-4977, (2015). https://doi.org/10.3390/ma8084961
[40] S. Abed, P. Laurens, C. Carrétéro, J. Deschamps and C. Duval, Diode laser welding of polymers: microstructures of the welded zones for polypropylene, in International Congress on Applications of Lasers & Electro-Optics, pp. 1499-1507, (2001). https://doi.org/10.2351/1.5059820